Journal of Food Engineering 100 (2010) 480–489

Contents lists available at ScienceDirect

Journal of Food Engineering

journal homepage: www.elsevier.com/locate/jfoodeng

# Preparation and characterization of bio-nanocomposite films based on soy protein isolate and montmorillonite using melt extrusion ☆

P. Kumar [a], K.P. Sandeep [a,*], S. Alavi [b], V.D. Truong [c], R.E. Gorga [d]

[a] Department of Food, Bioprocessing, and Nutrition Sciences, North Carolina State University, Raleigh, NC, USA
[b] Department of Grain Science and Industry, Kansas State University, Manhattan, KS, USA
[c] US Dept. of Agriculture, Agricultural Research Service, South Atlantic Area, Food Science Research Unit, Raleigh, NC, USA
[d] Department of Textile Engineering, Chemistry and Science, North Carolina State University, Raleigh, NC, USA

ARTICLE INFO

*Article history:*
Received 21 February 2010
Received in revised form 17 April 2010
Accepted 21 April 2010
Available online 23 May 2010

*Keywords:*
Bio-nanocomposite films
Soy protein isolate
Montmorillonite
Extrusion
Structural characterization
Mechanical properties
Water vapor permeability

ABSTRACT

The non-biodegradable and non-renewable nature of plastic packaging has led to a renewed interest in packaging materials based on bio-nanocomposites (biopolymer matrix reinforced with nanoparticles such as layered silicates). Bio-nanocomposite films based on soy protein isolate (SPI) and montmorillonite (MMT) were prepared using melt extrusion. Effects of the pH of film forming solution, MMT content, and extrusion processing parameters (screw speed and barrel temperature distribution) on the structure and properties of SPI–MMT bio-nanocomposite films were investigated. X-ray diffraction (XRD), transmission electron microscopy (TEM), and scanning electron microscopy (SEM) were used for structural characterization of the films. Properties of the films were determined by tensile testing, dynamic mechanical analysis (DMA), thermogravimetric analysis (TGA), and water vapor barrier measurement. The arrangement of MMT in the soy protein matrix ranged from exfoliated at lower MMT content (5%) to intercalated at higher MMT content (15%). There was a significant improvement in mechanical (tensile strength and percent elongation at break) and dynamic mechanical properties (glass transition temperature and storage modulus), thermal stability, and water vapor permeability of the films with the addition of MMT. The results presented in this study show the feasibility of using bio-nanocomposite technology to improve the properties of biopolymer films based on SPI.



## 1. Introduction

The non-degradable and non-renewable nature of plastic packaging has led to a renewed interest in packaging materials based on biopolymers derived from renewable sources. The use of biopolymer-based packaging materials can solve the waste disposal problem to a certain extent. Such biopolymers include those derived from naturally occurring proteins, cellulose, starches, and other polysaccharides and those synthesized chemically from naturally derived monomers such as lactic acid. Commercialization of biopolymer-based packaging materials has already started. Natureworks, LLC (Minnetonka, MN) manufactures polylactide from corn sugar. The polymer can be hydrolyzed back to lactic acid. Wal-Mart stores, Inc. is already using polylactide to package fresh-cut produce (Marsh and Bugusu, 2007). Currently, bio-based packaging materials constitutes about 1–2% of the food packaging market even though food packaging accounts for about 40% of the $460 billion global packaging industry (Jahangir and Leber, 2007). According to a report, the current capacity of bio-based packaging materials will increase from about 0.185 million tons annually to 0.545 million tons by 2012 (Schlechter, 2007).

The increased interest in bio-based packaging has resulted in the development of protein-based films from soy protein, whey protein, casein, collagen, corn zein, gelatin, and wheat gluten (Cuq et al., 1998). Among all the protein sources, soy proteins have attracted attention as a potential source for bio-based packaging materials because it has excellent film forming properties (Brandenburg et al., 1993; Gennadios et al., 1993; Zhang et al., 2001; Park et al., 2001; Mauri and Anon, 2006; Kurose et al., 2007). Soy protein isolate (SPI) is a commercial form of soy protein that contains more than 90% protein. 7S (β-conglycinin) and 11S (glycinin) fractions of soy proteins constitute about 90% of total protein. β-Conglycinin (molecular weight of 140–170 kDa) consists of three types of subunits with molecular weights of 58, 57, and 42 kDa.

☆ Paper nr FSR-09-37 of the Journal Series of the Department of Food, Bioprocessing, and Nutrition Sciences, North Carolina State University, Raleigh, NC 27695-7624.

* Corresponding author. Address: 129 Schaub Hall, Box 7624, North Carolina State University, Raleigh, NC 27695, USA. Tel.: +1 919 515 2957; fax: +1 919 515 7124.
*E-mail address:* kp_sandeep@ncsu.edu (K.P. Sandeep).

0260-8774/$ - see front matter © 2010 Elsevier Ltd. All rights reserved.
doi:10.1016/j.jfoodeng.2010.04.035

Glycinin (molecular weight of 340–375 kDa) consists of six acidic (35 kDa) and six basic (35 kDa) polypeptide chains which are linked together by disulfide bonds (Petruccelli and Anon, 1995).

SPI-based packaging films cannot meet the requirements of a cost-effective film with mechanical and barrier properties similar to those of plastics. Biopolymers made from SPI alone are extremely brittle. Plasticizers such as glycerol and polyethylene glycol impart flexibility to SPI-based biopolymer films. However, the use of plasticizers leads to significant decrease in tensile strength (TS) of the films (Wang et al., 1996). Soy protein-based films have been reported to have oxygen permeability (OP) similar to that of plastic films (Brandenburg et al., 1993). However, they have higher water vapor permeability (WVP) as compared to plastic films due to the hydrophilic nature of proteins. Therefore, research has been geared to develop techniques to improve mechanical and water vapor barrier properties of soy protein-based packaging materials.

Recently, a new class of materials represented by bio-nanocomposites (biopolymer matrix including proteins reinforced with nanoparticles such as montmorillonite) has proven to be a promising option in improving mechanical and barrier properties of biopolymers. The bio-nanocomposites consist of a biopolymer matrix reinforced with particles (nanoparticles) having at least one dimension in the nanometer range (1–100 nm) and exhibit much improved properties due to high aspect ratio and high surface area of nanoparticles (Ray and Bousmina, 2005; Rhim and Ng, 2007; Zhao et al., 2008). There are four possible arrangements of layered clays dispersed in a polymer matrix – phase separated or immiscible (microcomposite), intercalated, exfoliated, and disordered intercalated (partially exfoliated). Bio-nanocomposites can be obtained by several methods which include in situ polymerization, solution exfoliation, and melt intercalation (Dennis et al., 2001; Zeng et al., 2005).

The most common class of materials used as nanoparticles are layered clay minerals such as montmorillonite (MMT), hectorite, sapnotite, and laponite. These clay minerals have been proven to be very effective due to their unique structure and properties (Zeng et al., 2005). MMT has a very high elastic modulus (178 GPa) as compared to most biopolymers. The high value of elastic modulus enables MMT to improve mechanical properties of biopolymers by carrying a significant portion of the applied stress (Fornes and Paul, 2003).

Flexible bio-nanocomposites with improved properties can be obtained by reinforcing the SPI-plasticizer system with suitable filler materials such as MMT. Very few studies on SPI–MMT bio-nanocomposites have been reported in literature. Dean and Yu (2005) developed an effective method to exfoliate MMT lamellae in water using ultrasonic and prepared MMT-reinforced soy protein films plasticized by a mixture of water and glycerol. The ultrasonic treated bio-nanocomposite material exhibited an exfoliated structure and an improvement in tensile modulus and tensile strength of 84% and 47%, respectively. However, water barrier properties of the bio-nanocomposites were not reported. Rhim et al. (2005) prepared and studied the mechanical and water barrier properties of composite films of SPI with various clay minerals. The tensile strength of SPI-layered clay films increased by as much as 30% whereas the water vapor permeability decreased by 52%. Chen and Zhang (2006) prepared highly exfoliated and intercalated SPI–MMT nanocomposites by using the solution exfoliation method in a neutral aqueous medium and investigated the correlation between the microstructure and mechanical properties. Electrostatic attraction and hydrogen bonding at the interfaces of soy protein and MMT lead to good dispersion of MMT layers in the protein matrix. Highly exfoliated structure with 1–2 nm MMT layers dispersed in protein matrix resulted when the MMT content was less than 12% (w/w). Intercalated structure was predominant when the MMT content was more than 12%. The results also showed improvement in tensile strength (increase from 8.77 to 15.43 MPa) and thermal stability of SPI–MMT bio-nanocomposites.

Melt intercalation in an extruder is one of the most promising techniques for preparing bio-nanocomposites because of its ease and versatility. Layered clays (6–13 μm) are sheared and peeled apart into platelets (~1–10 nm) due to high shear mixing inside the extruder. These platelets are then mixed with the biopolymer matrix in molten state to achieve exfoliation (Dennis et al., 2001). Extrusion is one of the most important processing techniques to produce plastics on a commercial scale. Therefore, bio-nanocomposite films using extrusion will increase the potential for commercialization of these films. Extrusion processing parameters such as screw speed and barrel temperature distribution have an important influence on the structure and properties of nanocomposites. Increase in screw speed has been shown to result in better dispersion of nanoparticles in the polymer matrix. This behavior, observed for nanocomposites based on polyethylene (PE) and polypropylene (PP), is explained by breaking of agglomerates into smaller aggregates at high shear rates, corresponding to higher screw speeds. There are contradictory results in literature for the effect of barrel temperature distribution. Better dispersion of nanoparticles in PE at higher temperature has been reported. However, better dispersion of nanoparticles in PP was observed at lower temperature (Lertwimolnun and Vergnes, 2007).

The objective of this study was to prepare and characterize bio-nanocomposite films based on SPI and MMT using melt extrusion. Effects of the pH of film forming solution, MMT content, and extrusion processing parameters (screw speed and barrel temperature distribution) on the structure and properties (mechanical, dynamic mechanical, thermal stability, and water vapor permeability) of SPI–MMT bio-nanocomposite films were investigated.

## 2. Materials and methods

### 2.1. Materials

Soy protein isolate (Supro 760) with a protein content of 92.5% (dry basis) was obtained from Protein Technologies International (St. Louis, MO). Natural montmorillonite (Cloisite $Na^+$) was obtained from Southern Clay Products (Austin, TX). Cloisite $Na^+$ has a moisture content of 4–9% and a density of 2.86 g/cm$^3$. Glycerol, used as a plasticizer, was obtained from Fisher Scientific (Pittsburg, PA). Glycerol was chosen as the plasticizer because it is nontoxic whereas other potential polyhydric alcohols such as propylene glycol and ethylene glycol are toxic and hazardous (Wang et al., 1996).

### 2.2. Preparation of SPI–MMT nanocomposites

Process flow diagram for the preparation and characterization of soy protein isolate (SPI)-montmorillonite (MMT) bio-nanocomposite films is shown in Fig. 1. The formulation consisted of SPI (70–85%, dry basis), glycerol (15%, dry basis), and MMT (0–15%, dry basis). The ingredients were mixed and left at room temperature for 2 h for hydration. The mixture was subsequently extruded in a twin-screw co-rotating extruder (ZSK 26, Coperion Corp., Ramsey, NJ). The extruder had a five head barrel configuration with a screw diameter of 25 mm and length to diameter ratio (L/D) of 20. The extrudate was dried in an oven at 50 °C for 48 h. The dried extrudate was ground in a grinder (MicroMill, Bel-Art Products, Pequannock, NJ) for further testing and film casting.

### 2.3. Film casting

Bio-nanocomposite powders (4% w/v) and deionized water were mixed for 30 min at room temperature. pH of the suspension was adjusted to the desired value by adding either 1 M NaOH or

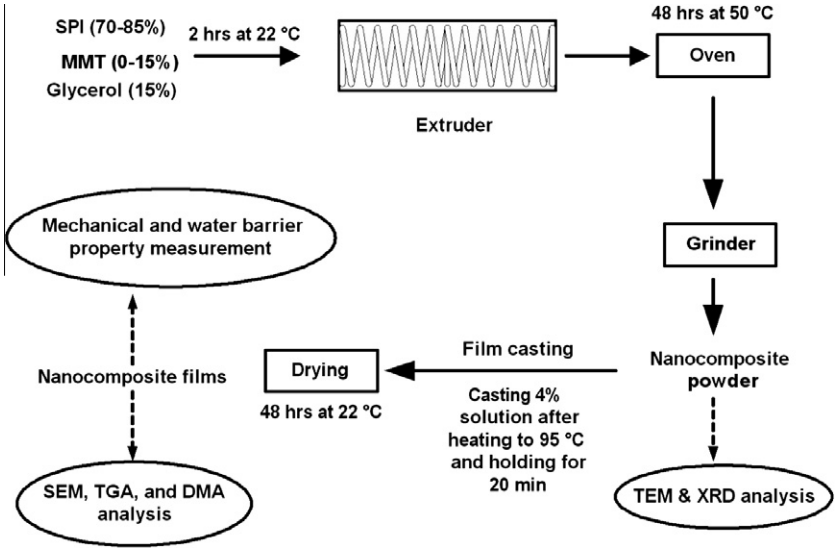


**Fig. 1.** Process flow diagram for the preparation and characterization of SPI–MMT bio-nanocomposite films.

1 M HCl solution. The suspension was heated to 95 °C and held at that temperature for 20 min with continuous stirring. Subsequently, the solution was cooled to 65 °C and 25 ml of the suspension was poured in 10 cm diameter petri dishes for casting nanocomposite films. The cast petri dishes were dried at ambient conditions for 48 h. The dried films were peeled off the petri dish and pre-conditioned at a temperature and relative humidity of 22 °C and 65%, respectively before further testing.

### 2.4. Structural characterization of SPI–MMT films

#### 2.4.1. X-ray diffraction (XRD)

X-ray diffraction studies of bio-nanocomposite powders were performed with a diffraction unit (MS Philips XLF ATPS XRD 100, Omni Scientific Instruments, Biloxi, MS) operating at 35 kV and 25 mA. The radiation was generated from a Cu-Kα ($\lambda = 0.154$ nm) source. The diffraction data was collected from $2\theta$ values of 2.5°–10° with a step size of 0.01°, where $\theta$ is the angle of incidence of the X-ray beam on the sample.

#### 2.4.2. Transmission electron microscopy (TEM)

The structure and morphology of bio-nanocomposite powders were visualized by a transmission electron microscope (Hitachi HF2000, Hitachi High-Technologies Europe GmbH, Krefeld, Germany) operating at 200 kV. Samples of bio-nanocomposite powders were prepared by suspending the powders in methanol. The suspension was sonicated for 5 min in an ultrasonic bath (Branson 1510, Branson Ultrasonics Co., Danbury, CT). A drop of the suspension was put on a fine-mesh carbon-coated TEM support grid (C-flat™, Protochips Inc., Raleigh, NC). After drying in air, the nanocomposite powder remained attached to the grid and was viewed under the transmission electron microscope.

#### 2.4.3. Scanning electron microscopy (SEM)

The morphology of the fracture surface (cross-sectional surface) of the bio-nanocomposite films were visualized using a field emission scanning electron microscope (JEOL 6400F, Japan Electron Optics Ltd., Tokyo, Japan) operating at 5 kV. Small pieces ($0.5 \times 0.5$ cm) of bio-nanocomposite films were frozen in liquid nitrogen, cut using a sharp razor blade, and mounted on specimen stubs with 2 sided carbon tape. The fracture surfaces of the films were sputter-coated with a thin layer (~8–10 nm) of gold–palladium (Au–Pd) using a sputter-coater (Hummer II, Anatech Ltd., Union City, CA). After coating, the samples were viewed under the scanning electron microscope.

### 2.5. Measurement of properties of SPI–MMT films

#### 2.5.1. Film thickness

Thickness of the films was measured at five different randomly selected locations using a digital micrometer (CO 030025, Marathon Watch Company Ltd., Ontario, Canada). The average value of the film thickness was used in determining mechanical properties, dynamic mechanical properties, and water vapor permeability.

#### 2.5.2. Mechanical properties

Tensile strength (TS) and percent elongation (%$E$) at break of the bio-nanocomposite films were determined by tensile testing using a Universal Testing Machine (model 5565, Instron, Corp., Canton, MA) equipped with a 5 kN static load cell according to the ASTM standard D882-02 (ASTM Standards, 2002). The length and width of the film samples were 5 cm and 2.5 cm, respectively. The initial grid separation was set at 2.5 cm and the cross-head speed was 50 cm/min. Stress vs. strain curves were plotted. Tensile strength was calculated by dividing peak load by initial specimen cross-sectional area. Percent elongation at break was calculated as the percentage change in length of the specimen between the grips. Three specimens of each sample were evaluated.

#### 2.5.3. Dynamic mechanical properties

The dynamic mechanical properties of bio-nanocomposite films were determined using a dynamic mechanical analyzer (Q800, TA Instruments, New Castle, DE). Dynamic mechanical analysis (DMA) was performed in tension mode at a frequency of 1 Hz and an amplitude of 15 μm. The length and width of the film samples were 4 cm and 0.6 cm, respectively. The samples were heated from 40 °C to 200 °C at a heating rate of 5 °C/min. The storage modulus ($E'$), loss modulus ($E''$), and loss tangent ($\tan\delta = E''/E'$) were recorded as a function of temperature. Glass transition temperature ($T_g$) was determined as the temperature at which tan δ attained its peak value.

*2.5.4. Thermal stability*

The thermal stability of bio-nanocomposite films were investigated using a thermogravimetric analyzer (Pyris 1 TGA, Perkin–Elmer, Shelton, CT). The mass of the sample used varied from 10 to 12 mg. Thermogravimetric analysis (TGA) was carried out separately under nitrogen and air flow. The temperature of the sample was increased from room temperature to 900 °C at a heating rate of 20 °C/min. Weight loss of the sample was measured as a function of temperature. Three parameters were determined from the TGA data: the temperature at 10% weight loss, the temperature at 50% weight loss, and the yield of charred residue at 850 °C.

*2.5.5. Water vapor permeability*

Water vapor permeability (WVP) of the bio-nanocomposite films was determined according to ASTM E96-05 (ASTM Standards, 2005). The sample film was cut into a circle of 8.75 cm diameter. The sample was placed on a test dish (8.2 cm in diameter and 1.9 cm in depth) filled with 50 ml deionized water to expose the films to 100% relative humidity. The test dishes were sealed and a turntable carrying 8 test dishes was rotated uniformly to ensure that all dishes were exposed to the same average ambient conditions during the test. The setup was subjected to a temperature and relative humidity of 22 °C and 65%, respectively. The test dishes were allowed to equilibrate for two hours before taking the initial weight. The final weight was taken after a 24 h interval. Water vapor transmission rate (WVTR) was calculated as (ASTM Standards, 2005):

$$\mathrm{WVTR} = \frac{G}{tA}, \tag{1}$$

where, $G$ is the change in weight (g), $t$ is the time (h), and $A$ is the area of the mouth of the test dish ($m^2$). Water vapor permeability (WVP) was calculated as (ASTM Standards, 2005):

$$\mathrm{WVP} = \frac{\mathrm{WVTR} \times L}{\Delta P}, \tag{2}$$

where, $L$ is the thickness of the test specimen (mm) and $\Delta P$ is the partial pressure difference of water vapor across the film. WVP of two specimens for each sample was calculated and reported.

*2.6. Design of experiments and statistical analysis*

Five different levels (3.0, 6.0, 7.5, 9.0, and 10.5) of pH at MMT contents of 0% and 5% were tested to optimize the pH of film forming solution. Subsequent experiments were carried out with the optimized pH value. Four different levels (0%, 5%, 10%, and 15%) of MMT content were used to study the effect of MMT content on the properties of bio-nanocomposite films. Screw speed and barrel temperature distribution used to study the effect of pH and MMT content were 100 rpm and $T_1$ (70, 90, 100, 110, and 90 °C), respectively. Two levels of screw speed ($N_1$: 50 rpm and $N_2$: 100 rpm) and three levels of barrel temperature distribution [$T_1$: (70, 90, 100, 110, and 90 °C); $T_2$: (80, 100, 110, 120, and 110 °C); $T_3$: (90, 110, 120, 130, and 120 °C)] were tested to study the effect of extrusion processing parameters on the properties of bio-nanocomposite films. A sample associated with a screw speed of $N_x$ and barrel temperature distribution of $T_y$ was coded as $N_xT_y$.

All experiments were performed in duplicate. Statistical analysis was performed using Minitab statistical software (Minitab Inc., State College, PA). Data were analyzed by either general linear model (GLM) or one-way analysis of variance (ANOVA). Differences at $P < 0.05$ were considered to be significant. Pair-wise comparison of all means was performed using the Fisher's least significant difference (LSD) method.

**Table 1**
Effects of pH and MMT content on mechanical properties (TS and %*E*) of SPI–MMT films.[A]

| | TS (MPa) | %*E* |
|---|---|---|
| SPI film (pH 7.5) | 1.86 ± 0.17[a] | 14.29 ± 1.17[a] |
| SPI film (pH 9.0) | 2.26 ± 0.48[a] | 11.85 ± 0.39[a] |
| SPI-5% MMT film (pH 7.5) | 4.79 ± 0.23[b] | 47.34 ± 3.56[b] |
| SPI-5% MMT film (pH 9.0) | 6.28 ± 0.88[b] | 64.60 ± 4.69[c] |

[A] Values are mean of two replicates ± standard deviation. Means in the same column followed by the same letter are not significantly different ($P > 0.05$).

## 3. Results and discussion

*3.1. Effect of pH of film forming solutions on the properties of films*

In the preliminary study, the effect of pH of film forming solutions on the mechanical and dynamic mechanical properties was investigated. There was no film formation at a pH value of 6.0. This pH was near the isoelectric point of soy protein isolate. It has been reported earlier that film formation does not take place near the isoelectric point of proteins (Brandenburg et al., 1993; Gennadios et al., 1993). Films formed at pH values of 3.0 and 10.5 were too brittle to be tested. Effect of pH and MMT content on mechanical properties (TS and %*E*) of SPI–MMT films is shown in Table 1. Effect of MMT content on TS was significant ($P = 0.001$) whereas the effect of pH on TS was not significant ($P = 0.061$). Films with MMT content of 5% had significantly higher TS than those with MMT content of 0%. Effect of MMT content and pH on %*E* was significant ($P < 0.05$). Analysis of variance using the general linear model showed that there was also a significant ($P < 0.05$) interaction effect of MMT content and pH on %*E*. At MMT content of 5%, films with higher %*E* were obtained at pH 9.0 as compared to those at pH 7.5.

Effect of temperature on tan $\delta$ of SPI–MMT films at pH values of 7.5 and 9.0 is shown in Fig. 2. Glass transition temperature ($T_g$), corresponding to the peak of the tan $\delta$ curve, was significantly ($P < 0.05$) affected by MMT content and pH. At a MMT content of 0%, $T_g$ increased from to 112.1 ± 2.3 °C to 119.7 ± 1.9 °C as the pH increased from 7.5 to 9.0. This might be attributed to increase in cross-linking of the films at pH 9 than those at pH 7.5. At a pH value of 9, $T_g$ increased from 119.7 ± 1.9 °C to 142.8 ± 2.0 °C as the MMT content increased from 0% to 5%. This is attributed to a reduction in the mobility of biopolymer chains of SPI in bio-nanocomposite films due to the interaction of SPI with MMT.

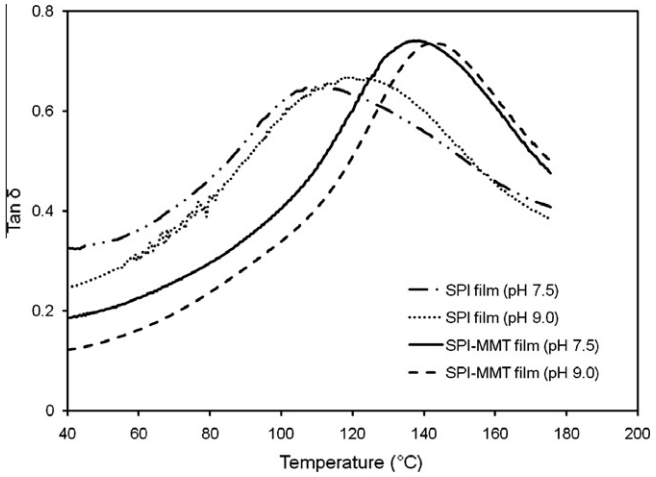


**Fig. 2.** Effect of temperature on tan $\delta$ of SPI–MMT films at different pH values.

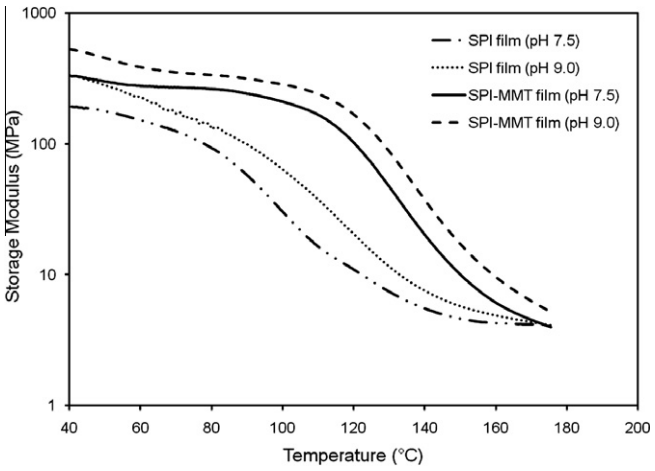


**Fig. 3.** Effect of temperature on storage modulus of SPI–MMT films at different pH values.

Effect of temperature on storage modulus ($E'$) of SPI–MMT films at pH values of 7.5 and 9.0 is shown in Fig. 3. Over the entire temperature range, $E'$ of the films at pH 9.0 was higher than those at pH 7.5. There was an increase of 175.3% in $E'$ of the films at 40 °C as the MMT content increased to 5% and pH changed from 7.5 to 9.0. This significant increase in $E'$ of films is attributed to the reduced mobility of biopolymer chains of SPI in bio-nanocomposite films. The increase in E' is also in agreement with the results of TS where TS increased with an increase in pH and MMT content. The films with MMT content of 5% had higher onset temperature for the abrupt decrease in the value of E' and the value of $E'$ reached a constant value in the plateau region at higher temperatures.

Based on the preliminary results, pH value of 9.0 was chosen as the optimum pH to obtain SPI–MMT films with desired mechanical and dynamic mechanical properties. pH value of 9.0 was used for the remaining part of the study.

### 3.2. Effect of MMT content on the structure of powders/films

XRD patterns of MMT and SPI–MMT bio-nanocomposite powders with 0%, 5%, 10%, and 15% MMT contents are shown in Fig. 4. Powders of MMT showed a diffraction peak at a $2\theta$ angle of 7.3°. Interlayer distance (d or d-spacing) between clay layers can be estimated from Bragg's equation (Kasai and Kakudo, 2005):

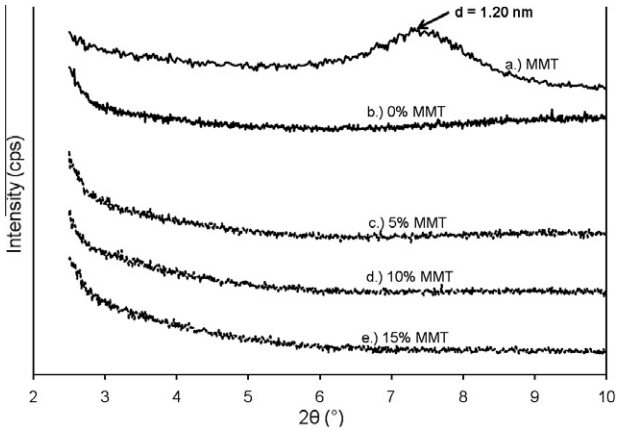


**Fig. 4.** XRD patterns of MMT and SPI–MMT bio-nanocomposites with different MMT contents.

$$d = \frac{\lambda}{2\sin\left(\frac{\pi\theta}{180}\right)}, \quad (3)$$

where, $\lambda$ is the wavelength of X-ray beam. The d-spacing of MMT corresponding to the diffraction peak was calculated to be 1.20 nm using Bragg's equation. This is in close agreement with the d-spacing value of 1.17 nm provided by the supplier. There was no diffraction peak in the $2\theta$ range of 2.5° to 10° for the bio-nanocomposites at all MMT contents. Absence of diffraction peaks for SPI–MMT bio-nanocomposites suggests that MMT layers have a d-spacing of at least 3.53 nm (corresponding to a $2\theta$ value of 2.5°) in SPI–MMT bio-nanocomposites with MMT content of up to 15%. Chen and Zhang (2006) reported a d-spacing value of 3 nm for SPI–MMT bio-nanocomposite powder prepared by a solution intercalation method at a MMT content of 16%. Higher d-spacing value reported in this study might have been achieved because of high shear mixing inside the twin-screw extruder. Morgan and Gilman (2003) showed that XRD by itself is insufficient to characterize the structure of nanocomposites for exfoliated and disordered intercalated arrangements. Therefore, XRD studies should always be complemented with microscopy techniques such as TEM or SEM.

TEM images of SPI–MMT bio-nanocomposite powders with 0%, 5%, 10%, and 15% MMT contents are shown in Fig. 5. The dark lines in the TEM images correspond to MMT platelets and the gap between two adjacent lines is the d-spacing. It can be seen from Fig. 5b that the MMT layers are exfoliated in bio-nanocomposites with MMT content of 5%. As MMT content increased to 10%, the arrangement of MMT changed from exfoliated to disordered intercalated (partially exfoliated). At MMT content of 15%, MMT layers are intercalated in bio-nanocomposites (Fig. 5d). However, d-spacing values, which ranged from 5 to 10 nm, were higher than the upper detection limit of XRD analysis (3.53 nm). This explains the absence of diffraction peaks for these bio-nanocomposites in the XRD analysis.

SEM images of the fracture surface (cross-sectional surface) of SPI–MMT bio-nanocomposite films with 0%, 5%, 10%, and 15% MMT contents are shown in Fig. 6. The white strands in the SEM images correspond to MMT platelets. At a MMT content of 5%, MMT platelets were well dispersed in the bio-nanocomposite film (Fig. 6b). This suggests exfoliation of MMT in the bio-nanocomposite film at a MMT content of 5%. The fracture surface of the films became rougher as the MMT content increased. Some aggregates of MMT were found at a MMT content of 15% (Fig. 6d).

Based on the XRD, TEM, and SEM results, it can be concluded that extrusion of SPI and MMT resulted in bio-nanocomposites with exfoliated structures at lower MMT content (5%) and intercalated structures at higher MMT content (15%).

### 3.3. Effect of MMT content on the properties of films

Mechanical properties (TS and %$E$) of SPI–MMT films with 0%, 5%, 10%, and 15% MMT contents were compared with those of other biopolymers, bio-nanocomposites, and plastic films (Table 2). SPI films had a TS of 2.26 ± 0.48 MPa and %$E$ of 11.85 ± 0.39. These values of TS and %$E$ are comparable to those for films based on soy protein and whey protein as reported in literature (Table 2). Films containing MMT had significantly higher TS as compared to that of SPI film. The value of TS increased from 2.26 ± 0.48 MPa to 15.60 ± 1.69 MPa as the MMT content increased from 0 to 15%. This is attributed to the high rigidity and aspect ratio of MMT and interaction of SPI with MMT. Films containing 5% MMT had significantly higher %$E$ as compared to that of SPI film. However, %$E$ decreased as the MMT content increased from 5% to 15%. This is attributed to the restricted motion of soy protein molecules in bio-nanocomposite films due to incorporation of MMT and interaction of SPI with MMT. TS values of films containing 10% and 15% MMT are

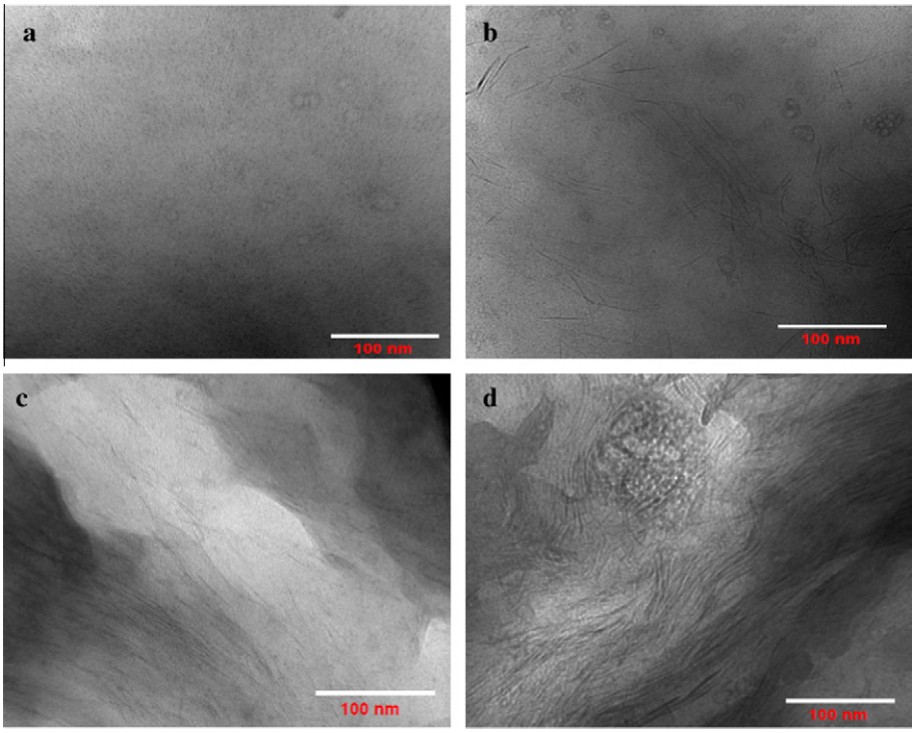


**Fig. 5.** TEM images of SPI–MMT bio-nanocomposites with (a) 0%, (b) 5%, (c) 10%, and (d) 15% MMT contents.

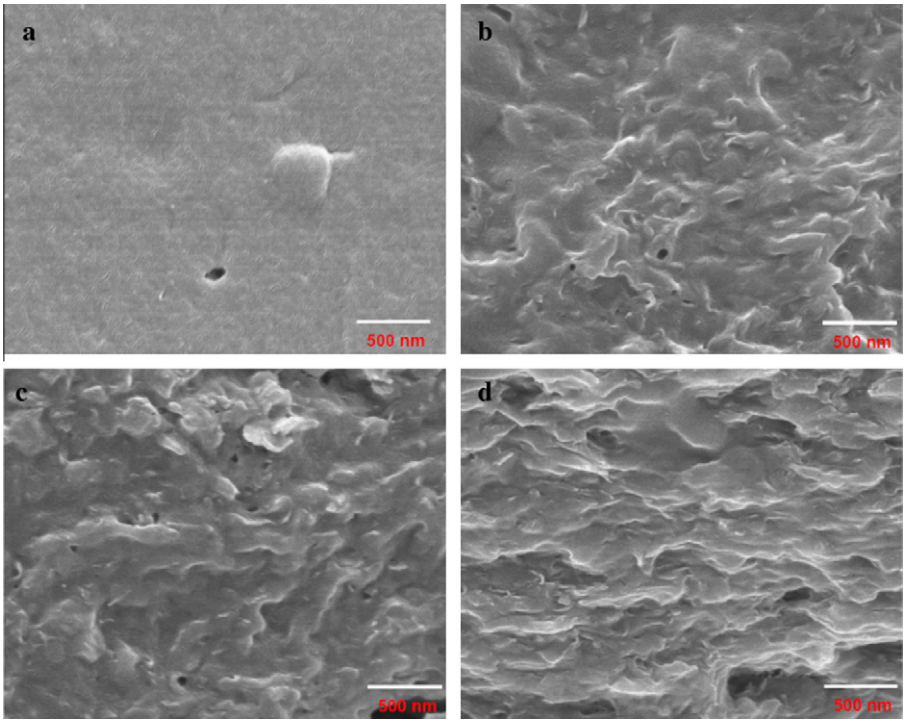


**Fig. 6.** SEM images of SPI–MMT bio-nanocomposite films with (a) 0%, (b) 5%, (c) 10%, and (d) 15% MMT contents.

comparable to those of low density polyethylene (LDPE) and polyvinylidene chloride (PVDC) which are currently used in food packaging applications. However, %*E* values for these plastic films range from 100–900% which is much higher than those for SPI–MMT films (11.85–64.60%). The lower value of %*E* might limit the application of these SPI–MMT films as food packaging materials. Mechanical properties of SPI–MMT films could further be improved by changing the type and content of plasticizer and incorporating other synthetic biodegradable polymers with improved properties. One such biodegradable polymer is polyvinyl alcohol (PVOH) which has higher TS (44–64 MPa) and %*E* (150–400%). Su et al. (2007) reported that %*E* of films based on blends of SPI and PVOH increased from 2.7% to 102% as the PVOH content increased from 0% to 40%.

**Table 2**
Comparison of mechanical properties (TS and %*E*) of SPI–MMT films[A] with other biopolymer, bio-nanocomposite, and plastic films.

| Films | TS (MPa) | %*E* |
|---|---|---|
| SPI | 2.26 ± 0.48[a] | 11.85 ± 0.39[a] |
| SPI-5% MMT | 6.28 ± 0.88[b] | 64.60 ± 4.69[b] |
| SPI-10% MMT | 12.62 ± 0.54[c] | 23.98 ± 5.02[c] |
| SPI-15% MMT | 15.60 ± 1.69[d] | 17.80 ± 2.27[ac] |
| Soy protein (Krochta (2002)) | 3–14 | 10–172 |
| Whey protein (Krochta (2002)) | 1–29 | 4–41 |
| Chitosan (Rhim et al. (2006)) | 32.9 | 54.6 |
| Chitosan-5% MMT (Rhim et al. (2006)) | 35.1 | 50.3 |
| Starch (Tang et al. (2008)) | 14.22 | 5.26 |
| Starch-6% MMT (Tang et al. (2008)) | 18.60 | 4.44 |
| Cellophane (Krochta (2002)) | 55–124 | 16–604 |
| Polylactic acid (PLA) (Rhim et al. (2009)) | 50.5 | 3 |
| Polyvinyl alcohol (PVOH) (Bohlmann (2005)) | 44–64 | 150–400 |
| Low density polyethylene (LDPE) (Selke (1997)) | 8.2–31.4 | 100–965 |
| Polypropylene (PP) (Selke (1997)) | 31–41.3 | 100–600 |
| Polyvinylidene chloride (PVDC) (Selke (1997)) | 19.3–34.5 | 160–400 |

[A] Values are mean of two replicates ± standard deviation. Means in the same column followed by the same letter are not significantly different ($P > 0.05$).

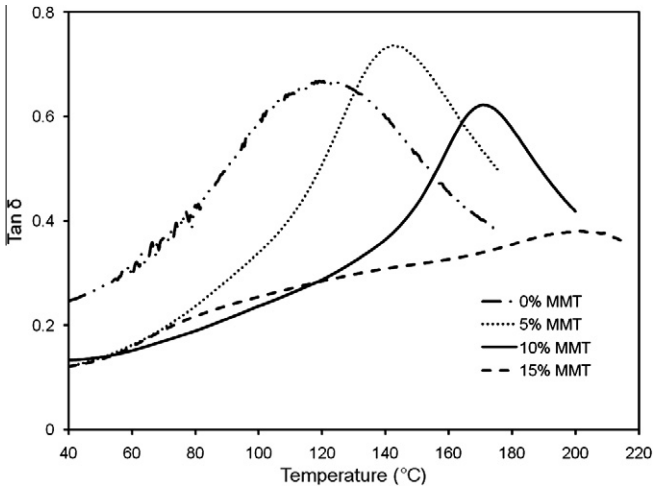


**Fig. 7.** Effect of temperature on tan $\delta$ of SPI–MMT films with different MMT contents.

Effect of temperature on tan $\delta$ of SPI–MMT films with 0%, 5%, 10%, and 15% MMT contents is shown in Fig. 7. There was a significant ($P < 0.05$) increase in glass transition temperature ($T_g$), depicted by the peak in the tan $\delta$ curve, with an increase in MMT content. SPI films had a $T_g$ of 119.7 ± 1.9 °C which is in the range of $T_g$ (111.9–150 °C) of SPI films as reported by Ogale et al. (2000). Glass transition temperature increased from 142.8 ± 2.1 °C to 199.5 ± 3.0 °C as the MMT content increased from 5 to 15%. This is attributed to reduced mobility of biopolymer chains of SPI in the bio-nanocomposite matrix. It can also be seen from Fig. 7 that the magnitude of tan δ peak value increases as MMT content increases to 5% and then decreases with further increase in MMT content. The area and magnitude of tan δ peak is an indication of the motion of polymer chains in amorphous phase (Yu et al., 2004). The broad peak with reduced magnitude at higher MMT contents can be attributed to restricted motion of biopolymer chains of SPI due to the interaction of SPI with MMT. It was also observed that there was a linear dependence of TS on $T_g$, given as:

$$TS = 0.1727 \times T_g - 18.17 \qquad (r^2 = 0.98) \tag{4}$$

Similar linear dependence of TS on $T_g$ of biopolymer films based on blends of PVOH and gelatin has been reported by Maria et al. (2008).

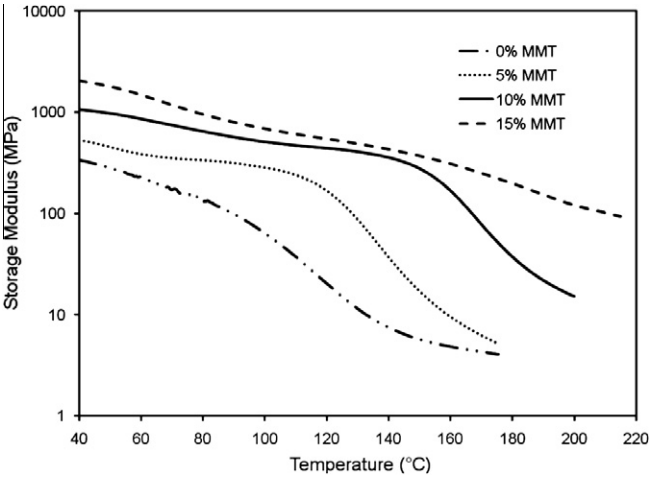


**Fig. 8.** Effect of temperature on storage modulus of SPI–MMT films with different MMT contents.

Effect of temperature on storage modulus (E') of SPI–MMT films with 0%, 5%, 10%, and 15% MMT contents is shown in Fig. 8. Over the entire temperature range, E' of SPI–MMT films was significantly ($P < 0.05$) higher than that of SPI films. Storage modulus of the films at 40 °C increased from 337 ± 31 MPa to 529 ± 24 MPa as the MMT content increased from 0% to 5%. Storage modulus of the films at 40 °C further increased to 2064 ± 54 MPa as the MMT content increased to 15%. This significant increase in E' of films is attributed to the reduced mobility of biopolymer chains of SPI in bio-nanocomposite films. The increase in E' is also in agreement with the results of tensile testing where TS increased with an increase in MMT content.

The thermal stability of SPI–MMT films was investigated using TGA separately under nitrogen and air flow (Figs. 9 and 10). It can be seen from Fig. 9 that there are 2–3 steps of thermal degradation of the films in the temperature range of 100–900 °C. The temperature range for the first step of thermal degradation is 100–150 °C. This corresponds to the loss of water from the films. The temperature range for the second step of thermal degradation is 300–400 °C. This corresponds to the decomposition of soy protein and loss of glycerol from the films. Under air flow, there is an additional third step of thermal degradation in the temperature range of 500 to 800 °C. This might be due to oxidation of partially

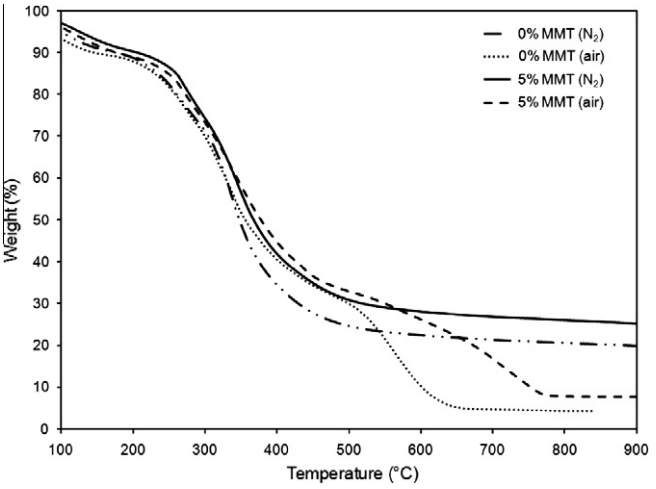


**Fig. 9.** TGA curves of SPI–MMT bio-nanocomposite films under $N_2$ and air flow.

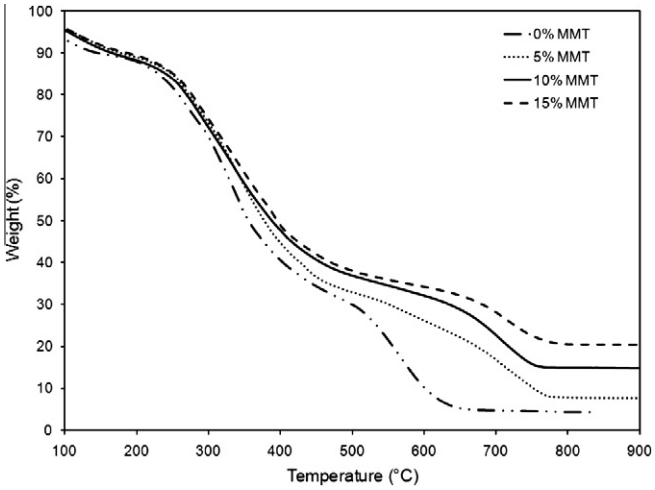


**Fig. 10.** TGA curves of SPI–MMT bio-nanocomposite films with different MMT contents under air flow.

**Table 3**
Comparison of water vapor permeability (WVP) of SPI–MMT films[A] with other biopolymer, bio-nanocomposite, and plastic films.

| Films | WVP (g-mm/(m$^2$-h-kPa)) |
|---|---|
| SPI | 3.80 ± 0.11[a] |
| SPI-5% MMT | 2.96 ± 0.10[b] |
| SPI-10% MMT | 2.49 ± 0.08[c] |
| SPI-15% MMT | 2.17 ± 0.06[d] |
| Soy protein | 1.62–6.42 (Krochta (2002)) |
| Whey protein | 1.58–12.12 (Krochta (2002)) |
| Chitosan | 4.72 (Rhim et al. (2006)) |
| Chitosan-5% MMT | 3.52 (Rhim et al. (2006)) |
| Starch | 1.61 (Tang et al. (2008)) |
| Starch-6% MMT | 1.06 (Tang et al. (2008)) |
| Cellophane | 0.05–0.25 (Kamper and Fennema (1984)) |
| Polylactic acid (PLA) | 0.06 (Rhim et al. (2009)) |
| Polyvinyl alcohol (PVOH) | 3.15 (Lange and Wyser (2003)) |
| Low density polyethylene (LDPE) | 0.001 (Krochta (2003)) |
| Polypropylene (PP) | 0.02–0.04 (Lange and Wyser (2003)) |
| Polyvinylidene chloride (PVDC) | 0.01 (Lange and Wyser (2003)) |

[A] Values are mean of two replicates ± standard deviation. Means in the same column followed by the same letter are not significantly different ($P > 0.05$).

decomposed soy protein under air flow. Similar results for different types of bio-nanocomposite films have been reported (Wang et al., 2006; Tunc et al., 2007).

TGA curves of SPI–MMT bio-nanocomposite films with different MMT contents under air flow are shown in Fig. 10. As the MMT content increased, the bio-nanocomposite films exhibited a significant delay in weight loss at temperatures greater than 400 °C. The temperature at 50% weight loss (during TGA) increased from 355.5 ± 2.2 °C to 377.3 ± 2.6 °C with an increase in MMT content from 0 to 5%. The temperature at 50% weight loss further increased to 395.4 ± 3.2 °C as the MMT content increased to 15%. This can be attributed to the fact that MMT platelets reduce the rate of diffusion of volatile decomposition products out of the bio-nanocomposite bulk. MMT platelets create a tortuous pathway for volatile decomposition products to diffuse out of the bio-nanocomposite matrix. This increases the effective path length for diffusion, thus reducing the rate of diffusion (Chen et al., 2001). The mechanism for improved thermal stability has also been attributed to the thermal insulation behavior of MMT and changes in the dynamics of molecular motion in bio-nanocomposites (Leszczynska and Pielichowski, 2008). After decomposition at 850 °C, the films yielded charred residue proportional to their clay content. The yield of charred residue at 850 °C increased from 4.2 ± 0.3% to 7.8 ± 0.4% with an increase in MMT content from 0 to 5%. The yield of charred residue at 850 °C further increased to 20.5 ± 0.4% as MMT content increased to 15%. This increased yield of charred residue can be attributed to the addition of MMT which is thermally stable up to a temperature of 900 °C. Kim and White (2005) reported that MMT (Cloisite $Na^+$) yields more than 85% solid residue at 800 °C.

Water vapor permeability (WVP) of SPI–MMT films with 0%, 5%, 10%, and 15% MMT contents was compared with that of other biopolymers, bio-nanocomposites, and plastic films (Table 3). Higher WVP is one of the major limitations in using protein-based films as food packaging materials. Therefore, reduction in WVP is desirable for potential applications in food packaging. SPI films had a WVP of 3.80 ± 0.11 g-mm/(m$^2$-h-kPa) which is comparable to the WVP of other biopolymer films based on protein, chitosan, and starch as reported in literature (Table 3). Films containing MMT had significantly ($P < 0.05$) lower WVP as compared to that of SPI film. WVP for films with 5% MMT reduced by 22.1%. This reduction is comparable to the results with chitosan-MMT (25.4% reduction) and starch-MMT (34.2% reduction) reported in literature (Table 3). The reduction in WVP by MMT has been attributed to the creation of a tortuous pathway for water vapor to diffuse out of the bio-nanocomposite matrix. This increases the effective path length for diffusion of water vapor molecules, thus reducing WVP (Zeng et al., 2005). WVP reduced by as much as 42.9% as the MMT content increased from 0% to 15%. However, the WVP values for SPI–MMT films are still much higher as compared to those for plastics such as low density polyethylene (LDPE), polypropylene (PP), polyvinylidene chloride (PVDC). This might limit the application of these bio-nanocomposite films to packaging of high moisture foods such as fresh fruits and vegetables.

### 3.4. Effect of extrusion parameters on the properties of films

Effect of extrusion processing parameters (screw speed and barrel temperature distribution) on mechanical properties (TS and %*E*) of SPI–MMT films with MMT content of 5% is shown in Table 4. There was a significant ($P < 0.05$) increase in TS of the films with an increase in screw speed and barrel temperature. Improved TS at higher screw speed can be attributed to better dispersion of MMT. Higher shear rate, corresponding to higher screw speed, can break bigger agglomerates of MMT into smaller aggregates. Improved TS at higher barrel temperature can be attributed to a decrease in viscosity with increase in temperature. The stress required to break MMT aggregates is reduced as the viscosity decreases (Lertwimolnun and Vergnes, 2007). An increase in barrel temperature can also increase the extent of protein denaturation. Denatured proteins will have more biopolymer chains available for network formation, resulting in films with improved TS. Analy-

**Table 4**
Effect of extrusion processing parameters on mechanical properties (TS and %*E*) of SPI–MMT films with MMT content of 5%.[A]

| Extrusion processing parameters | TS (MPa) | %*E* |
|---|---|---|
| $N_1T_1$ | 4.63 ± 0.46[a] | 11.24 ± 1.08%[a] |
| $N_1T_2$ | 5.24 ± 0.14[b] | 20.43 ± 2.18%[a] |
| $N_1T_3$ | 6.49 ± 0.12[b] | 25.20 ± 3.67%[a] |
| $N_2T_1$ | 6.28 ± 0.88[b] | 64.60 ± 4.69%[b] |
| $N_2T_2$ | 8.29 ± 0.71[c] | 38.00 ± 6.07%[b] |
| $N_2T_3$ | 9.25 ± 0.34[c] | 41.00 ± 5.00%[b] |

$N_1$ = 50 rpm, $N_2$ = 100 rpm.
$T_1$: (70, 90, 100, 110, and 90 °C).
$T_2$: (80, 100, 110, 120, and 110 °C).
$T_3$: (90, 110, 120, 130, and 120 °C).
[A] Values are mean of two replicates ± standard deviation. Means in the same column followed by the same letter are not significantly different ($P > 0.05$).

sis of variance using the general linear model showed that the interaction effect of screw speed and barrel temperature distribution on TS was insignificant ($P > 0.05$). There was a significant ($P < 0.05$) increase in $\%E$ of the films with an increase in screw speed. Effect of barrel temperature distribution and interaction effect of barrel temperature distribution and screw speed on $\%E$ were insignificant ($P > 0.05$). It can be concluded that higher screw speed and barrel temperature are desirable to prepare films with higher TS and $\%E$.

Effect of temperature on tan δ of SPI–MMT films with MMT content of 5% at different extrusion processing parameters is shown in Fig. 11. There was a significant ($P < 0.05$) increase in glass transition temperature with an increase in screw speed and barrel temperature. At a barrel temperature distribution of $T_1$, $T_g$ increased from 134.3 ± 1.1 °C to 142.8 ± 2.0 °C as the screw speed increased from $N_1$ (50 rpm) to $N_2$ (100 rpm). At a screw speed of $N_2$, $T_g$ increased from 142.8 ± 2.0 °C to 158.6 ± 0.8 °C as the barrel temperature distribution changed from $T_1$ (70, 90, 100, 110, and 90 °C) to $T_3$ (90, 110, 120, 130, and 120 °C). This can be attributed to better dispersion of MMT and network formation at higher screw speed and barrel temperature. It can also be seen from Fig. 11 that the magnitude of tan δ peak decreases with an increase in barrel temperature. This result supports the fact that more biopolymer chains of soy protein were involved in network formation with MMT at higher barrel temperature.

Effect of temperature on storage modulus ($E'$) of SPI–MMT films with MMT content of 5% at different extrusion processing parameters is shown in Fig. 12. Over the entire temperature range, $E'$ of films at higher screw speed and higher barrel temperature was higher than that of films at lower screw speed and lower barrel temperature. There was an increase of 51.2% in $E'$ of the films at 40 °C as the screw speed increased from 50 to 100 rpm. The corresponding increase was 139.3% as the barrel temperature distribution changed from $T_1$ to $T_3$. The increase in $E'$ is also in agreement with the results of tensile testing where TS increased with an increase in screw speed and barrel temperature.

Effect of extrusion processing parameters (screw speed and barrel temperature distribution) on water vapor permeability (WVP) of SPI–MMT films with MMT content of 5% is shown in Table 5. Analysis of variance using the general linear model showed that the effect of screw speed on WVP was significant ($P < 0.05$). The effect of barrel temperature distribution and interaction effect of barrel temperature distribution and screw speed on WVP were insignificant ($P > 0.05$).

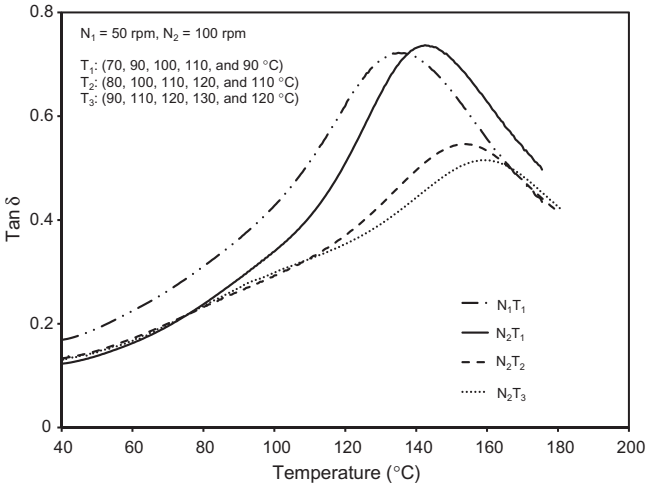


**Fig. 11.** Effect of temperature on tan $\delta$ of SPI–MMT films at different extrusion processing parameters.

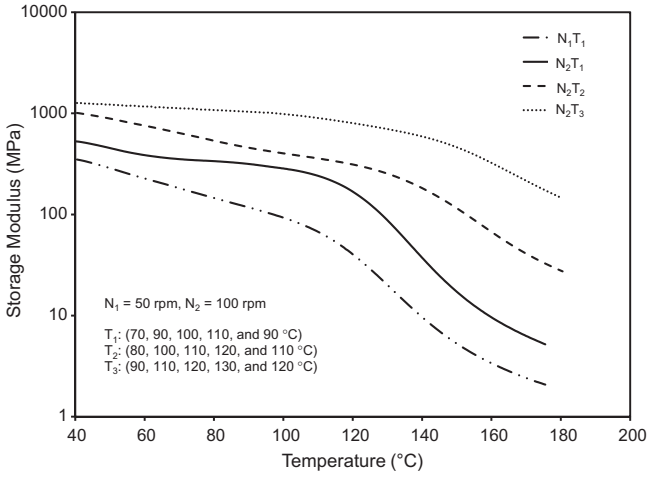


**Fig. 12.** Effect of temperature on storage modulus of SPI–MMT films at different extrusion processing parameters.

**Table 5**
Effect of extrusion processing parameters on WVP of SPI–MMT films with MMT content of 5%.[A]

| Extrusion processing parameters | WVP (g-mm/(m$^2$-h-kPa)) |
|---|---|
| $N_1T_1$ | 3.19 ± 0.11$^a$ |
| $N_1T_2$ | 3.09 ± 0.10$^a$ |
| $N_1T_3$ | 3.13 ± 0.08$^a$ |
| $N_2T_1$ | 2.96 ± 0.10$^b$ |
| $N_2T_2$ | 2.91 ± 0.11$^b$ |
| $N_2T_3$ | 2.76 ± 0.07$^b$ |

$N_1$ = 50 rpm, $N_2$ = 100 rpm.
$T_1$: (70, 90, 100, 110, and 90 °C).
$T_2$: (80, 100, 110, 120, and 110 °C).
$T_3$: (90, 110, 120, 130, and 120 °C).
[A] Values are mean of two replicates ± standard deviation. Means in the same column followed by the same letter are not significantly different ($P > 0.05$).

## 4. Conclusions

Bio-nanocomposite films based on soy protein isolate (SPI) and montmorillonite (MMT) with improved properties were prepared using melt extrusion. The arrangement of MMT in the bio-nanocomposite matrix ranged from exfoliated at lower MMT content (5%) to intercalated at higher MMT content (15%). There was a significant improvement in mechanical (tensile strength and percent elongation at break) and dynamic mechanical properties (glass transition temperature and storage modulus), thermal stability, and water vapor permeability of the films with the addition of MMT. Properties of the SPI–MMT films were significantly affected by the pH of film forming solutions, MMT content, and extrusion processing parameters (screw speed and barrel temperature distribution). The results presented in this study show the feasibility of using bio-nanocomposite technology to improve the properties of biopolymer films based on SPI. The same technology can also be applied to biopolymers based on starch and other proteins. These bio-nanocomposite films could potentially be used for packaging of high moisture foods such as fresh fruits and vegetables to replace some of the existing plastics such as low density polyethylene (LDPE) and polyvinylidene chloride (PVDC). However, there is a need to further improve the properties of these SPI–MMT films for commercial application.

## Acknowledgments

Support for the research study undertaken here, resulting in the publication of paper No FSR-09-37 of the Journal Series of the Dept.

of Food, Bioprocessing, and Nutrition Sciences, NCSU, Raleigh, NC 27695-7624 from USDA-NRICGP Grant No 2008-01503, titled: Development of cross-linked bio-nanocomposite packaging films with enhanced barrier and mechanical properties, is gratefully acknowledged. We would also like to thank Birgit Anderson, Gail Liston, Roberto Garcia, Chuck Mooney, Jonathan Pierce, and Sharon Ramsey for their assistance in conducting the experiments.

The use of trade names in this publication does not imply endorsement by the North Carolina Agricultural Research Service of the products named nor criticism of similar ones not mentioned.

## References


ASTM Standards, 2002. D882-02. Standard test Method for Tensile Properties of Thin Plastic Sheeting. Philadelphia, PA.

ASTM Standards, 2005. E96-05. Standard Test Methods for Water Vapor Transmission of Materials. Philadelphia, PA.

Bohlmann, G.M., 2005. General characteristics, processability, industrial applications and market evolution of biodegradable polymers. In: Bastioli, C. (Ed.), Handbook of Biodegradable Polymers. Rapra Technology Ltd., Shropshire, UK, pp. 183–218.

Brandenburg, A.H., Weller, C.L., Testin, R.F., 1993. Edible films and coatings from soy protein. Journal of food Science 58, 1086–1089.

Chen, P., Zhang, L., 2006. Interaction and properties of highly exfoliated soy protein/montmorillonite nanocomposites. Biomacromolecules 7, 1700–1706.

Chen, G., Liu, S., Chen, S., Qi, Z., 2001. FTIR spectra, thermal properties, and dispersibility of a polystyrene/montmorillonite nanocomposite. Macromolecular Chemistry and Physics 202, 1189–1193.

Cuq, B., Gontard, N., Guilbert, S., 1998. Proteins as agricultural polymers for packaging production. Cereal Chemistry 75 (1), 1–9.

Dean, K., Yu, L., 2005. Biodegradable protein–nanoparticles composites. In: Smith, R. (Ed.), Biodegradable Polymers for Industrial Applications. Woodhead Publishing Ltd., UK, pp. 289–312.

Dennis, H.R., Hunter, D.L., Chang, D., Kim, S., White, J.L., Cho, J.W., Paul, D.R., 2001. Effect of melt processing conditions on the extent of exfoliation in organoclay-based nanocomposites. Polymer 42, 9513–9522.

Fornes, T.D., Paul, D.R., 2003. Modeling properties of nylon 6/clay nanocomposites using composite theories. Polymer 44, 4993–5013.

Gennadios, A., Brandenburg, A.H., Weller, C.L., Testin, R.F., 1993. Effect of pH on properties of wheat gluten and soy protein isolate films. Journal of Agricultural and Food Chemistry 41, 1835–1839.

Jahangir, S., Leber, M.J., 2007. Biodegradable food packaging: an environmental imperative. Industry report. pp. 1–20.

Kamper, S.L., Fennema, O., 1984. Water vapor permeability of edible bilayer films. Journal of Food Science 49, 1478–1481.

Kasai, K., Kakudo, M., 2005. X-ray Diffraction by Macromolecules. Springer, New York. p. 504.

Kim, Y., White, J.L., 2005. Formation of polymer nanocomposites with various organoclays. Journal of Applied Polymer Science 96, 1888–1896.

Krochta, J.M., 2002. Proteins as raw materials for films and coatings: definitions, current status, and opportunities. In: Gennadios, A. (Ed.), Protein-based Films and Coatings. CRC Press, Boca Raton, FL, pp. 1–41.

Krochta, J.M., 2003. Package permeability. In: Heldman, D.R. (Ed.), Encyclopedia of Agricultural, Food, and Biological Engineering. Marcel Dekker, Inc., NY, p. 720–726.

Kurose, T., Urman, K., Otaigbe, J.U., Lochhead, R.Y., Thames, S.F., 2007. Effect of uniaxial drawing of soy protein isolate biopolymer films on structure and mechanical properties. Polymer Engineering and Science 47 (4), 374–380.

Lange, Y., Wyser, Y., 2003. Recent innovations in barrier technologies for plastic packaging – a review. Packaging Technology and Science 16, 149–158.

Lertwimolnun, W., Vergnes, B., 2007. Influence of screw profile and extrusion conditions on the microstructure of polypropylene/organoclay nanocomposites. Polymer Engineering and Science 47 (12), 2100–2109.

Leszczynska, A., Pielichowski, K., 2008. Application of thermal analysis methods for characterization of polymer/montmorillonite nanocomposites. Journal of Thermal Analysis and Calorimetry 93 (3), 677–687.

Maria, T.M.C., de Carvalho, R.A., Sobral, P.J.A., Habitante, A.M.B.Q., Feria, J.S., 2008. The effect of the degree of hydrolysis of the PVA and the plasticizer concentration on the color, opacity, and thermal and mechanical properties of films based on PVA and gelatin blends. Journal of Food Engineering 87, 191–199.

Marsh, K., Bugusu, B., 2007. Food packaging – roles, materials, and environmental issues. Journal of Food Science 72 (3), R39–R55.

Mauri, A.N., Anon, M.C., 2006. Effect of solution pH on solubility and some structural properties of soybean protein isolate films. Journal of the Science of Food and Agriculture 86, 1064–1072.

Morgan, A.B., Gilman, J.W., 2003. Characterization of polymer-layered silicate (clay) nanocomposites by transmission electron microscopy and X-ray diffraction: a comparative study. Journal of Applied Polymer Science 87, 1329–1338.

Ogale, A.A., Cunningham, P., Dawson, P.L., Acton, J.C., 2000. Viscoelastic, thermal, microstructural characterization of soy protein isolate films. Journal of Food Science 65 (4), 672–679.

Park, S.K., Rhee, C.O., Bae, D.H., Hettiarachchy, N.S., 2001. Mechanical properties and water vapor permeability of soy protein films affected by calcium salts and glucono-$\delta$-lactone. Journal of Agricultural and Food Chemistry 49, 2308–2312.

Petruccelli, S., Anon, M.C., 1995. Soy protein isolate components and their interactions. Journal of Agricultural and Food Chemistry 43, 1762–1767.

Ray, S.S., Bousmina, M., 2005. Biodegradable polymers and their layered silicate nanocomposites: in greening the 21st century materials world. Progress in Materials Science 50, 962–1079.

Rhim, J.W., Ng, P.K.W., 2007. Natural biopolymer-based nanocomposite films for packaging applications. Critical Reviews in Food Science and Nutrition 47 (4), 411–433.

Rhim, J.W., Lee, J.H., Kwak, H.S., 2005. Mechanical and barrier properties of soy protein and clay mineral composite films. Food Science and Biotechnology 14, 112–116.

Rhim, J.W., Hong, S.I., Park, H.M., Ng, P.K.W., 2006. Preparation and characterization of chitosan-based nanocomposite films with antimicrobial activity. Journal of Agricultural and Food Chemistry 54, 5814–5822.

Rhim, J.W., Hong, S.K., Ha, C.S., 2009. Tensile, water vapor barrier and antimicrobial properties of PLA/nanoclay composite films. LWT Food Science and Technology 42, 612–617.

Schlechter, M., 2007. Biodegradable polymers. Report code PLS025C. <http://bccresearch.com/report/PLS025C.html> (accessed 20.02.10).

Selke, S.E.M., 1997. Understanding Plastics Packaging Technology. Hanser Publication, New York, p. 206.

Su, J.F., Huang, Z., Liu, K., Fu, L.L., Liu, H.R., 2007. Mechanical properties, biodegradation, water vapor permeability of blend films of soy protein isolates and poly(vinyl alcohol) compatibilized by glycerol. Polymer Bulletin 58, 913–921.

Tang, X., Alavi, S., Herald, H.J., 2008. Barrier and mechanical properties of starch–clay nanocomposite films. Cereal Chemistry 85 (3), 433–439.

Tunc, S., Angellier, H., Cahyana, Y., Chalier, P., Gontard, N., Gastaldi, E., 2007. Functional properties of wheat gluten/montmorillonite nanocomposite films processed by casting. Journal of Membrane Science 289, 159–168.

Wang, S., Sue, H.J., Jane, J., 1996. Effects of polyhydric alcohols on the mechanical properties of soy protein plastics. Journal of Macromolecular Science, Part A 33 (5), 557–569.

Wang, S., Chen, L., Tong, Y., 2006. Structure-property relationship in chitosan-based biopolymer/montmorillonite nanocomposites. Journal of Polymer Science: Part A: Polymer Chemistry 44, 686–696.

Yu, Z.Z., Yan, C., Yang, M., Mai, Y.W., 2004. Mechanical and dynamic mechanical properties of nylon 66/montmorillonite nanocomposites fabricated by melt compounding. Polymer International 53, 1093–1098.

Zeng, Q.H., Yu, A.B., Lu, G.Q., Paul, D.R., 2005. Clay-based polymer nanocomposites: research and commercial development. Journal of Nanoscience and Nanotechnology 5, 1574–1592.

Zhang, J., Mungara, P., Jane, J., 2001. Mechanical and thermal properties of extruded soy protein sheets. Polymers 42, 2569–2578.

Zhao, R., Torley, P., Halley, P.J., 2008. Emerging biodegradable materials: starch- and protein-based bio-nanocomposites. Journal of Materials Science 43, 3058–3071.